New trends in flood risk analysis: working with 2D flow models, laser DEM and a GIS environment

P. ARCHAMBEAU, B. DEWALS, S. ERPICUM, S. DETREMBLEUR & M. PIROTTON
Laboratory of Applied Hydrodynamics and Hydraulic Constructions, University of Liege, Belgium

Second author: Research Fellow of the National Fund for Scientific Research (Belgium)

ABSTRACT: This paper outlines the integration of new and accurate laser DEM into the determination of floodplains. Global and robust GIS environment is absolutely necessary to manage this very large amounts of topographic data. The development and interaction of 2D flow models, simplified or not, ensures to offer more accurate and flexible physically based tools to the decision-makers.

1 INTRODUCTION

Floods control, risk mapping and more generally river management are topics on which a wide range of decision makers focus a permanently increasing attention. The first step in flood hazard analysis and management, prior to any mitigation policy, is a thorough understanding and assessing of the level of risk. Though lots of work has been carried out for decades in the field, a genuinely reliable and efficient modelling of the corresponding flows remains a challenge. In spite of improved computation capacities, collecting, handling and validating large sets of topographic data as well as simulation results are still challenging tasks for hydro-modellers and practitioners.

The present paper covers a description and a detailed comparison of two state-of-the-art numerical models to be used as strategic tools in the process of flood risk assessment and mitigation. The first one is a 2D model for hydrodynamics, simplified according to the diffusive assumption (DM), quickly generating initial flow fields for the second one, a complete model based on the shallow water equations (SWE).

Those two models are integrated in the software package WOLF, which has been developed for almost ten years at the University of Liege. WOLF includes a complete set of numerical models for simulating free surface flows (process-oriented and spatially distributed hydrology [1], 1D and 2D hydrodynamics [2, 3], sediment transport [4, 5], air entrainment [6] …) as well as optimisation algorithms. This optimisation tool, based on the innovative Genetic Algorithms, allows an objective calibration of friction coefficients [7].

A user-friendly GIS interface, entirely designed and implemented by the authors, makes the pre- and post-processing operations very convenient. Import and export operations are easily feasible from and to various classical GIS tools. Different layers of maps can be handled to analyse information related to topography, ground characteristics, vegetation density and hydrodynamic fields.

The validation of the model has been performed continuously for many years and is still running. Two cases studies on Belgian rivers are presented to illustrate inundation applications in a urban area.

2 MATHEMATICAL MODEL DESCRIPTION

The SWE model simulates any steady or unsteady situation, possibly taking into consideration air transport or sediment-laden flows, in Cartesian or curvilinear coordinates. It is in addition coupled to a turbulence model based on the Prandtl mixing length concept. The DM model is restricted to a specific range of Froude and kinematic numbers, but requires significantly less CPU resources.

In the shallow-water approach (SWE) the only assumption states that velocities normal to a main flow direction are smaller than those in the main flow direction. As a consequence the pressure field is found to be almost hydrostatic everywhere. In the diffusive model (DM) a similar depth-averaging operation is combined to the following hypothesis: the purely advective terms can be neglected. As a consequence the free surface slope is simply balanced by the friction term.

The divergence form of the SWE include the mass balance:

$$\frac{\partial H}{\partial t}+\frac{\partial q_i}{\partial x_i}=0 \qquad (1)$$

and the momentum balance:

$$\underbrace{\left[\frac{\partial q_i}{\partial t}+\frac{\partial}{\partial x_i}\left(\frac{q_i q_j}{h}\right)\right]}_{\text{inertia terms}}+gh\left(S_{fi}+\frac{\partial H}{\partial x_i}\right)=0; \quad j=1,2 \quad (2)$$

where Einstein's convention of summation over repeated subscripts has been used. H represents the free surface elevation, h is the water height, q_i designates the specific discharge in direction i and S_{fi} is the friction slope.

The *diffusive assumption* leads to a considerable simplification of the momentum equations:

$$S_{fi}=-\frac{\partial H}{\partial x_i}. \quad (3)$$

A friction law is needed for closure of both the SWE and the DM models. Its general formulation can be stated as a relation between the discharge, the water height and the slope:

$$q=\alpha h^{\chi} S_f^{\gamma}=\alpha h^{\chi}\left(\frac{\partial H}{\partial s}\right)^{\gamma}, \quad (4)$$

where α, γ and χ are coefficients suitable for the description of floodplain flows.

A more detailed description of the mathematical formulation can be found in the recent paper by Archambeau *et al* [3].

3 NUMERICAL IMPLEMENTATION

A finite volume scheme is used in all models to ensure exact mass conservativity. An upwind scheme is exploited for space discretization of the SWE model and extended to the DM.

An implicit pseudo-time integration scheme, suitable for solving non-transient problems, is implemented in the SWE model. In the DM model the GMRES or Conjugate Gradients (CG) algorithms are used for evaluating iteratively the solution of the symmetric linearized system.

3.1 *Space discretization and boundary conditions*

An original upwind scheme is applied for space discretization of the complete set of equations. The stability of this second order upwind scheme has been demonstrated through a theoretical study of the mathematical system as well as a von Neumann stability analysis. Much care has been taken to handle correctly the source terms representing topography gradients. A fitted spatial upwinded scheme is developed similarly to the previously described DM.

The models allow the user to specify any inflow discharge as an upstream boundary condition (BC). The downstream boundary condition can be a free surface elevation, a water height, a Froude number or even no specified condition if the outflow regime is supercritical (SWE only).

3.2 *Resolution of the DM model*

The primary goal of the diffusive formulation is the quick computation of steady-state approximate solutions. Those first estimations of the final solution are intended to serve as fairly good initial condition for the complete SWE model.

A first approach for solving the DM might be a pseudo-time evolution, starting from a user-defined initial condition. In order to prevail the possibility of using large time steps, this pseudo-time integration would need to be performed in an implicit way.

A second approach is to disregard the time derivative term and to solve a non-linear system of time independent equations. Both methods are obviously very similar if the time step becomes very large. Various iterative techniques are available for solving such very large linear systems. Among them are the methods « by point », such as Jacobi, Gaus-Seidel,… [8, 9] or full implicit such as ADI [10-14], GMRES [15], CG [16-19].

3.3 *Time integration for the SWE model*

An implicit pseudo-time integration scheme, suitable for solving steady-state problems, is implemented in the SWE model. This technique allows much larger time steps than those acceptable for an explicit time integration. On the other hand the resolution procedure is more intricate. A Newton method is exploited to solve the large non-linear system. The successive linearized systems are solved with the powerful GMRES algorithm, which is advantageously coupled to a preconditioner. For this purpose an Incomplete LU decomposition is applied. The Switched Evolution-Relaxation technique by Van Leer has been used to continuously optimise the time step.

In the DM model the GMRES or CG algorithms are also used for evaluating iteratively the solution of the symmetric linearized system. In both cases the resolution procedure represents a very challenging step because of the complexity of a cost-effective evaluation of the Jaobian matrix. WOLF performs this job effectively, by storing only non-zero elements and their location in the large sparse matrix.

3.4 *Friction modelling*

River and floodplain flows are mainly driven by topography gradients and by friction effects. The total friction includes three components: bottom friction (drag and roughness), wall friction and internal friction.

The bottom friction is classically modelled thanks to an empirical law, such as the Manning formula.

The DM and SWE models allow the definition of a spatially non uniform roughness coefficient. This parameter can thus easily be distributed as a function of soil properties, vegetation and sub-grid bed forms.

The friction along vertical boundaries, such as bank walls, is introduced thanks to a physically-based model developed by the authors. This modification of the classical friction law presents the advantage of leading to a correct hydraulic radius of the 2D cross-section in case of sufficiently shallow flows.

The internal friction is properly reproduced by the turbulence model.

3.5 *More features of the numerical codes*

In addition an automatic mesh refinement is used to enhance the convergence rate towards accurate steady-state solutions [3]. The computations are performed on several successive grids, first very coarse and then gradually refined. The hydrodynamic fields are almost stabilized when the computer code automatically jumps onto the next grid. This fully automatic method considerably reduces the number of cells in the first grids. Then, the successive so-called initial solutions are interpolated from the coarser towards the finer grid in terms of both water heights and discharges.

In case of an explicit pseudo-time evolution: the stable time step is significantly larger since it depends linearly on the size of the mesh. For an implicit evolution, the benefits of the quadratic convergence are reached since the initial solution is sufficiently close to the steady state solution. In spite of extra computation time to re-mesh and linearly interpolate the initial solution the overall CPU time saving is clearly appealing.

4 LASER DEM

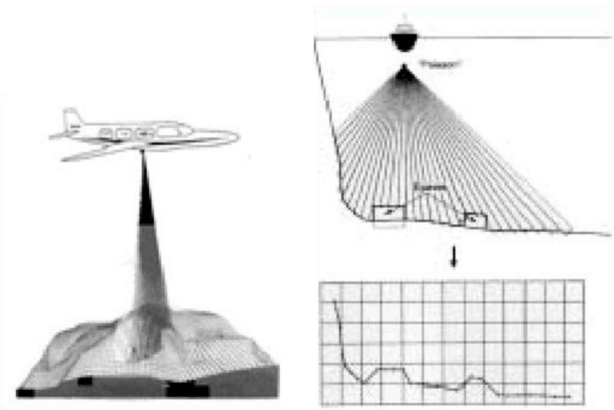

Figure 1. Principle of the DEM acquisition by airborne laser and echo-sonar ship

Very recently, the Belgian Ministry of Facilities and Transport (MET) and most particularly the Service of Hydrology Studies (SETHY) acquired a very accurate DEM on the floodplains in the whole Walloon Region.

A method of airborne laser was used for the proximity inundation zones of the entire rivers network. An echo-sonar was applied for measuring the bathymetry of the main channel, exclusively on navigable rivers (Fig. 1).

Consequently, the poor and inaccurate 3D information that has been available for many years, 30 m square and an error of several meters in altitude, is replaced by an exceptional DEM since the precision in altitude is 15 cm and, on top of that, the information density is one point per square meter.

To illustrate the accuracy of the DEM, (Figs. 2 and 3) two comparisons of data on the same regions are presented, the towns of Bethane and Eupen (Belgium).

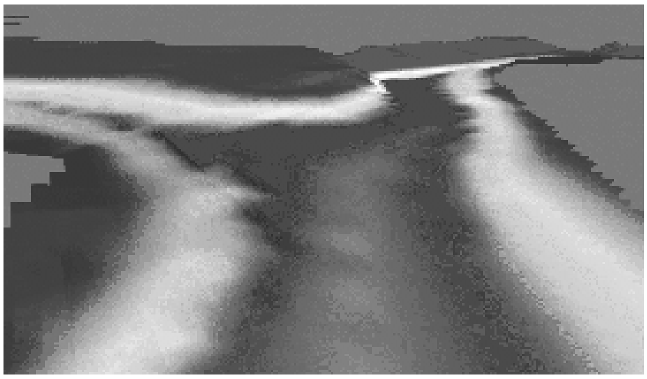

Figure 2a. Béthane: IGN topography (digitalized contour line map)

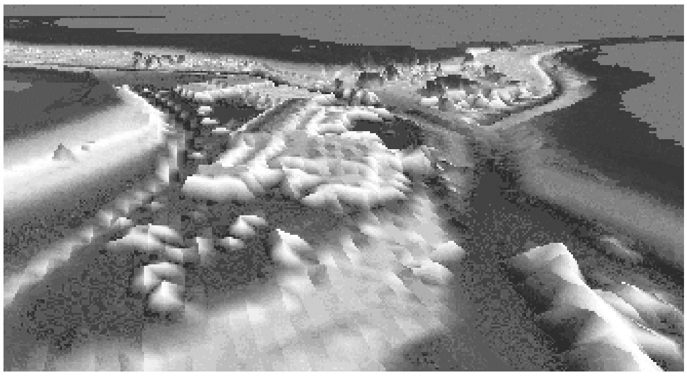

Figure 2b. Béthane: laser data including buildings

Generally, specific features of flows in urban area (such as blockage by buildings, slowing down of the wave front propagation, etc) were taken into account by a local modification of the roughness coefficient. While, with this new set of topographic data, irregularities of the topography influence directly the inundation flows. This permits to refocus the roughness coefficient to more proper physical values.

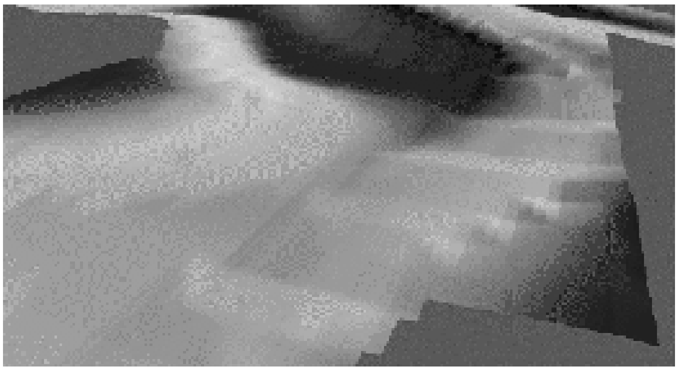

Figure 3a. Eupen: IGN topography (digitalized contour line map)

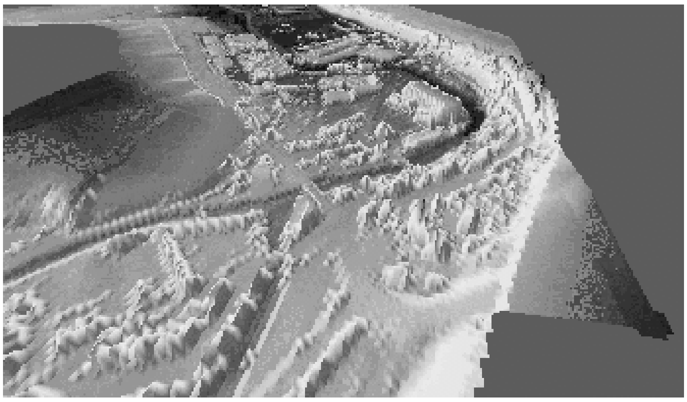

Figure 3b. Eupen: laser data including buildings

5 GIS ENVIRONMENT

Management and operations on such a large set of data requires a robust and efficient pre- and post-processing. A GIS environment, entirely designed and implemented by the authors, performs this tools. Several databases containing topographic data, pictures of historic floods, characteristics of structures along the rivers (dams, bridges, weirs, …) are stored on a single data server with their geographic coordinates to be easily downloaded by any modeller.

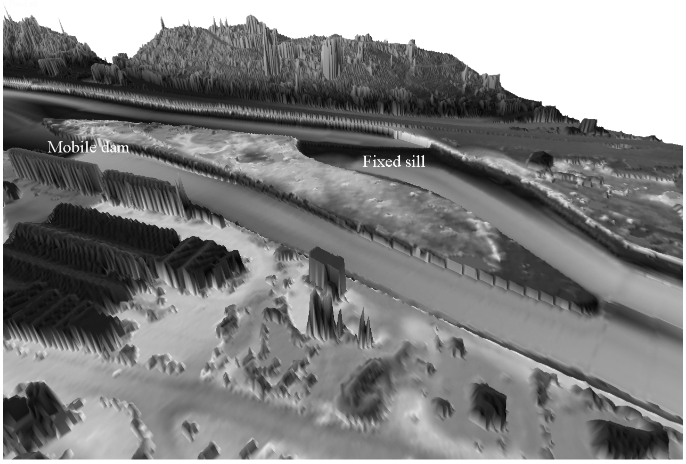

Figure 4. Example of DEM interpolation of the river bed and aggregation with the airborne laser data (river Ourthe, Tilff; Belgium).

A difficult task for the pre-processing is the interpolation of the minor river bed when no distributed data are available. It's the case on the non-navigable rivers where the airborne laser is the only source of the DEM. In fact, the laser beam doesn't cross the water surface. Therefore, the only available information are based on cross sections and thus must be interpolated in 3D to recompose a global DEM. Original methods were developed by Detrembleur [20] to fulfil this job and are implemented in the WOLF package.

6 CASES STUDIES

6.1 *Flood induced inundation on the river Ourthe*

The first case proposed is a flood event on the river Ourthe that occurs 14 February 2002 (study commissioned by the MET-SETHY).

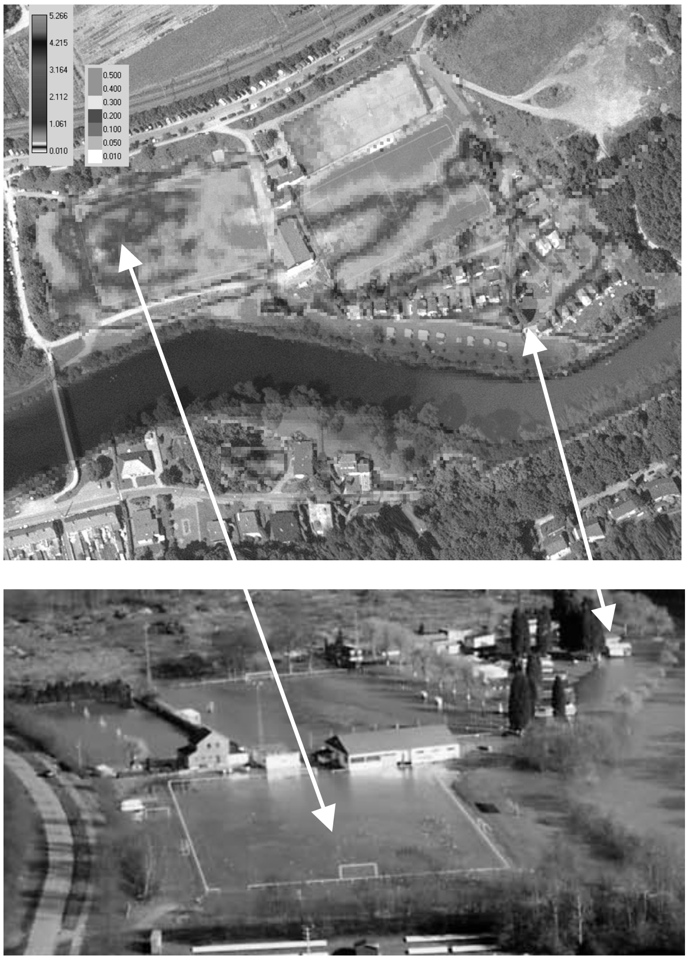

Figure 5. Comparison between water heights and aerial picture of the flood event (football field).

Characteristics of the simulation are :

- Discharge: 570 m³/s
- Length of the real computed river: 7,35 km
- Total number of computations cells: 300.000
- Uniform size of the cells: 2 x 2 m
- Two hydraulic structures: a mobile dam and a fixed sill

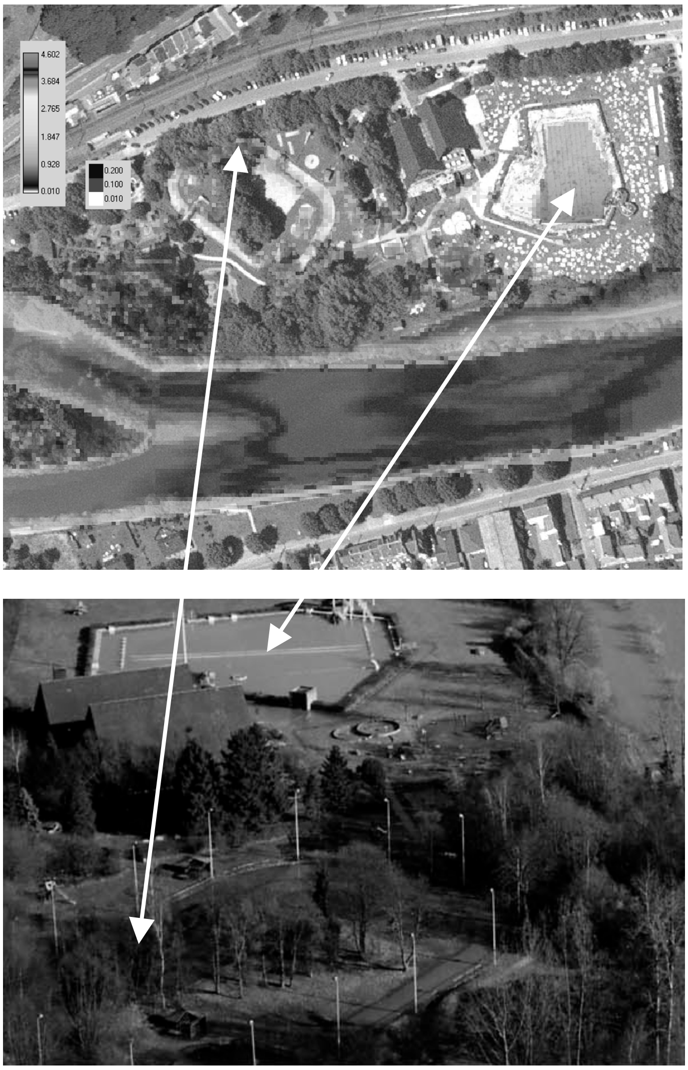

Figure 6. Comparison between water heights and aerial picture of the flood event (water-pool of the “Prés de Tilff”).

In this case, there were discrepancies between the first simulation and the real observations. Actually, the interpolation of the main river bed was computed based on cross sections taken in ’70 years. Actually, major modifications of this bed were realized to mitigate floods in the town of Tilff. The right bank was newly designed to a vertical wall when it was computed with a slope of 4:4. A complete dredging was performed too.

After the introduction of the different modifications in the topography, the results improved significantly as demonstrate the comparisons between numerical water heights and aerial pictures of the floods (Fig. 5-6)

6.2 *Flood inundation on the river Lesse*

The second case presented in this paper consists in the verification of the works protecting from floods in Han-sur-Lesse on the river Lesse, Belgium (study commissioned by DGRNE, Walloon Region).

This town, which attracts tourists, is located at the downstream of geological caves that divert the free surface flow of the Lesse trough underground flow. A maximum discharge of about 25 m³/s can pass by this way. The rest is forced to return to the historical bed.

A first stage was the building of a diversion channel to increase the natural discharge capacity of the river. A side-weir creates a separation between the two channels. Thus, the normal discharge only flows in the natural river. In addition, a second stage consists in the building of walls and small dyke to prohibit the overflow in the urban zone.

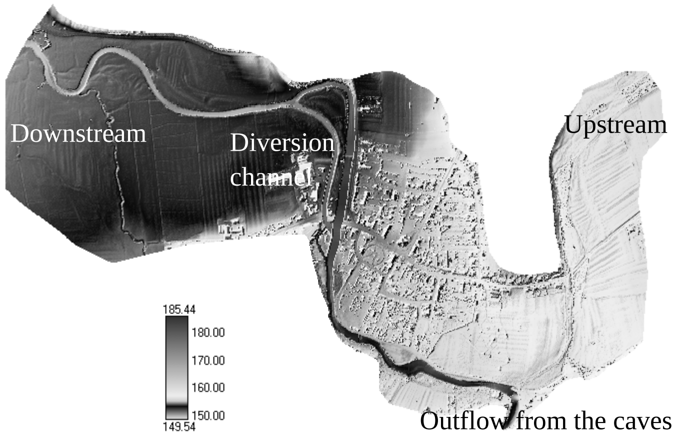

Figure 7. General topography of Han-sur-Lesse.

Figure 8. Enlargement of the downstream topography

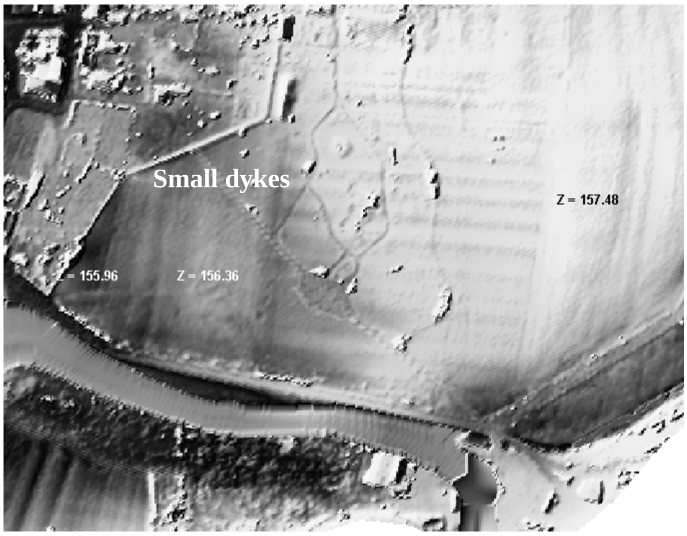

Figure 9. Enlargement of the topography around the exit of the caves.

Figures 8 and 9 illustrate the precision of the laser DEM. The drainage channels of farm fields, residual erosion of historical floodings, current small dyke and the interpolated topography of the main river bed can be observed.

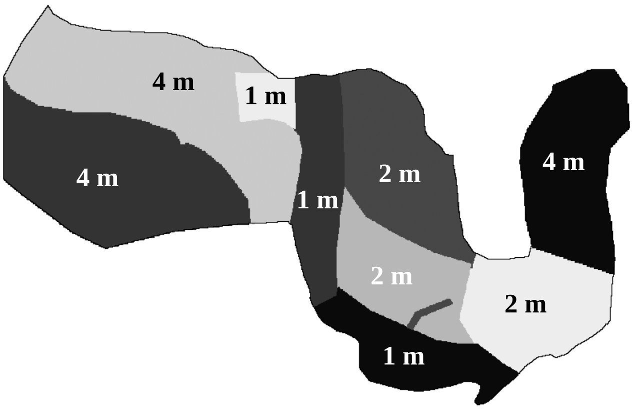

Figure 10. Multiblocs discretization.

Characteristics of the simulations are :

- Discharge: 150 m³/s
- Length of the real computed river: 4 km
- Total number of computations cells: 450.000
- Variable size of cells (Fig. 10)
- Hydraulic structures: a mobile dam and several fixed sills

A multibloc discretization is used in this problem to limit the total computation time. The finest information is conserved along the river trough the town but a progressive increase in the cells size is performed to words the extremities of the computation domain to ensure evanescent boundary conditions.

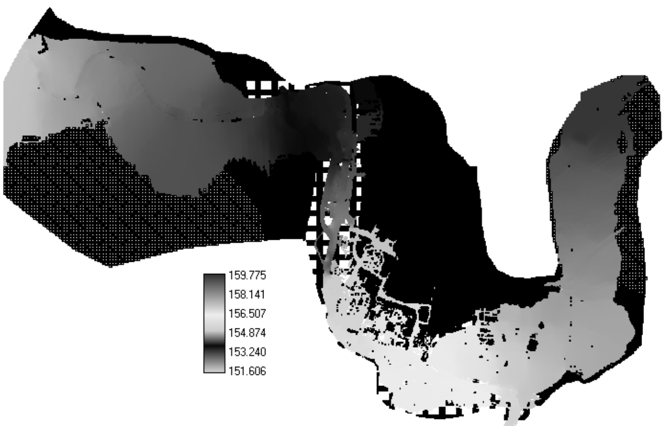

Figure 11. Free surface elevation for the flood of January 2003.

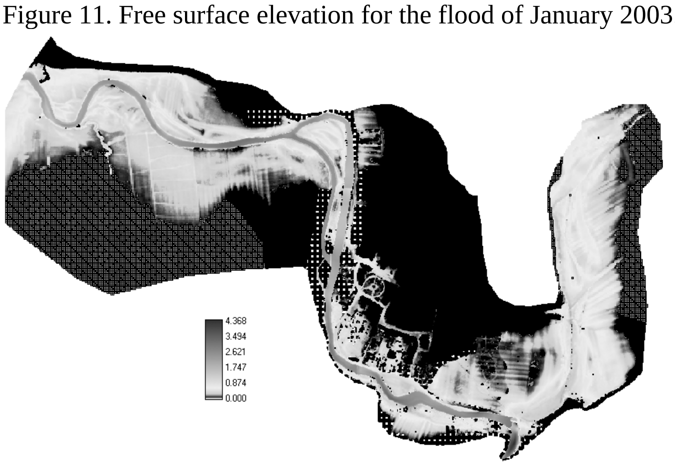

Figure 12. Water heights for the flood of January 2003.

The reference event dates from Jannuary 2003 because it's the only flood after the building of the diversion channel. Figures 11 and 12 illustrate the results in terms of free surface elevation and water heights. A good concordance is obtained between computed results and field observations, and thus both in extension of the flood and in water heights.

An observation of the results in terms of Froude numbers (Fig. 13) permits to indentify a critical section, just before the side-weir, in an obvious place. The real nature of the problem consists in a rise of the bottom topography due to an outcrop. This critical section reduces significantly the favourable effect of the stage 1 on the upstream. Furthermore, stage 2 doesn't modify this place bacause the buildings just stop at the upstream. Thus, recommendations were made to the manager to extent the works to redraw this portion of river.

The check of the stage 2 consists in a simulation where the town is untouchable by the floods. Thus, impermeable boundary conditions are applied on the outline of the town. A comparison of the final water heights with the heights of walls and dykes concludes to a good design of the works

Observation (cm)	*Computed (cm)*
82	86
5	15-30 center of street
25	5 along the houses
20	30
94	95
113	117
100	100

Table 1. Comparison of water height for the flood of January 2003

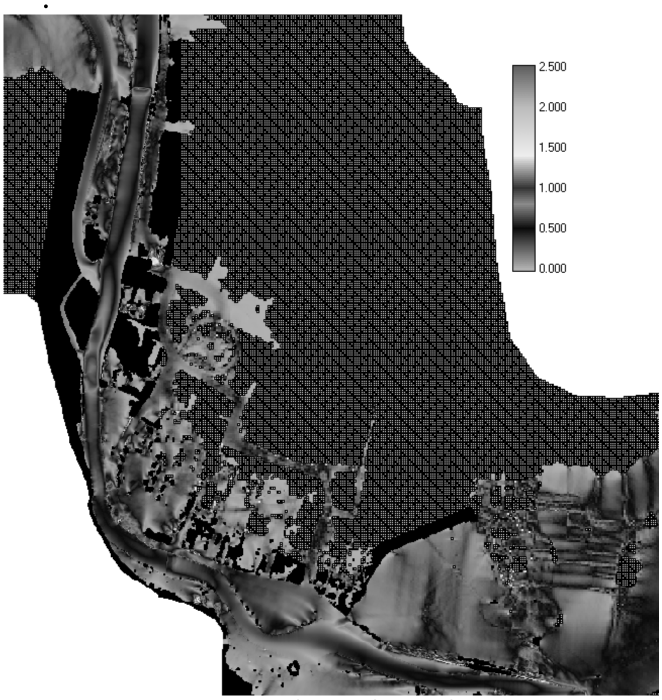

Figure 13. Froude number for the flood of January 2003.

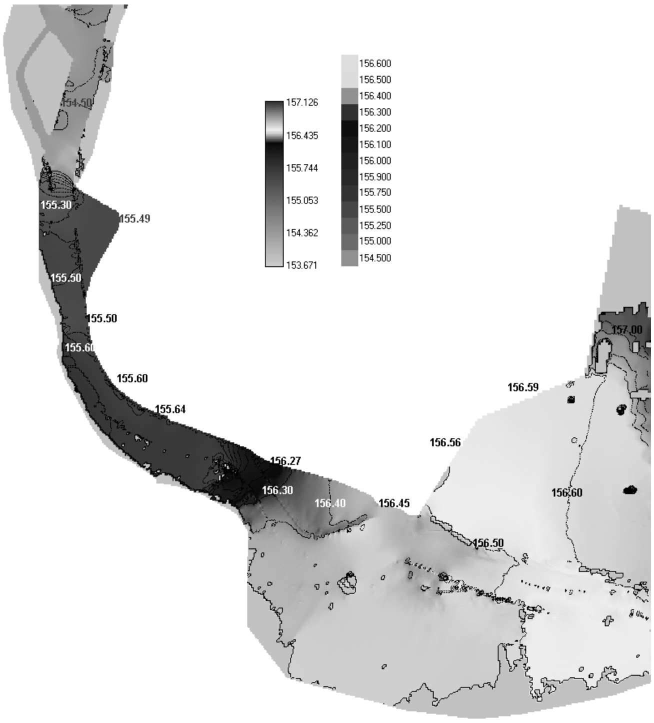

Figure 14. Free surface elevation after the building of stage 2 (m)

7 CONCLUSION

The present paper offers a comprehensive comparison between both numerical models (DM and SWE) for very practical applications such as floodplains modelling and inundation maps plotting. The key advantages brought by the GIS environment are also illustrated, focusing on the major contemporary requirements of decision makers in the field of flood control.

Further research is currently undertaken for investigating sediment transport effects and their simulation.

8 BIBILOGRAPHY

[1] Archambeau, P., et al. Impact studies and water management with WOLFHYDRO : a new physically based hydrological solver. in International Symposium on Environmental Hydraulics. 2001. Arizona State University, USA.

[2] Mouzelard, T., et al. Water management of large dams. in International Symposium on Environmental Hydraulics. 2001. Arizona State University, USA.

[3] Archambeau, P., et al., A set of efficient numerical tools for floodplain modeling, in Shallow Flows, G.H. Jirka and W.S.J. Uijttewaal, Editors. 2003, IfH & TU Delft: Delft. p. 141-158.

[4] Dewals, B., et al. Coupled computations of highly erosive flows with WOLF software. in 5th International Conference on Hydro-Science & -Engineering. 2002. Warsaw University of Technology.

[5] Dewals, B., et al., Dam-break hazard mitigation with geomorphic flow computation, using WOLF 2D hydrodynamic software, in Risk Analysis III, C.A. Brebbia, Editor. 2002, WIT Press.

[6] André, S., et al. Quasi 2D-numerical model of aerated flow over stepped chutes. in XXX IAHR Congress. 2003. Thessaloniki, Greece: IAHR.

[7] Erpicum, S., et al., Optimising a cascade of hydroelectric power stations with the WOLF package, in Water Ressources Management, C.A. Brebbia, Editor. 2003, WIT Press. p. 65-74.

[8] Hirsch, C., Numerical Computation of Internal and External Flows, Computational Methods for Inviscid and Viscous Flows. Vol. Volume 2. 1990: Wiley. 691.

[9] Young, D.M., Iterative solution of large linear system. Englewood Cliffs. 1971, New York: Academic Press.

[10] Kim, S. and J. Douglas, Fractional time-stepping methods for unsteady flow problems, http://citeseer.nj.nec.com/382490.html

[11] Malhotra, S., C. Douglas, and M. Schultz, Parameter choices for ADI-like methods on parallel computers, 2000, http://citeseer.nj.nec.com/11073.html

[12] Douglas, J. and S. Kim, On accuracy of alternating direction implicit methods for parabolic equations, 1999, http://citeseer.nj.nec.com/douglas99accuracy.html

[13] Molls, T. and G. Zhao, Depth-averaged simulations of supercritical flow in channel with wavy sidewall. Journal of Hydraulic Engeneering, 2000. 126(6): p. 437-445.

[14] Panagiotopoulos, A. and J. Soulis, Implicit bidiagonal scheme for depth-averaged free-surface flow equations. Journal of Hydraulic Engeneering, 2000. 126(6): p. 425-436.

[15] Saad, Y. and M. Schultz, GMRES : A generalized minimal residual algorithm for solving non-symmetric linear system. SIAM Journal of Scientific and Statistical Computing, 1986. 7.

[16] Jones, M. and P. Plassman, An improved incomplete Cholesky factorization. 1991, Mathematics and Computer Science Division, Argonne National Laboratory: Illinois. p. 12,

[17] White, D., Solution of Capacitance systems using incomplete Cholesky fixed point iteration. Journal for Numerical Methods in Engeneering, 1998.

[18] Lin, C.-J. and M. J, Incomplete Cholesky factorizations with limited memory, 1997,

[19] CACR, C.f.a.c.r., NAG Libraries. 2000, http://www.cacr.caltech.edu.

[20] Detrembleur, S., Elaboration d'outils intégrés de gestion des données topographiques et morphologiques pour la modélisation des crues et inondations, in Applied Hydrodynamics and Hydraulic Constructions. 2003, University of Liège: Liège. p. 110,